Lawrence Berkeley Laboratory
UNIVERSITY OF CALIFORNIA

Materials & Chemical Sciences Division

The Reaction of Ground State and Electronically Excited Sodium Atoms with Methyl Bromide and Molecular Chlorine

P.S. Weiss, J.M. Mestdagh, H. Schmidt, M.H. Covinsky, and Y.T. Lee

November 1990

DISCLAIMER

THE REACTION OF GROUND STATE AND ELECTRONICALLY EXCITED SODIUM ATOMS WITH METHYL BROMIDE AND MOLECULAR CHLORINE

P.S. Weiss, J.M. Mestdagh, H. Schmidt, M.H. Covinsky, and Y.T. Lee

Department of Chemistry
University of California

and

Chemical Sciences Division
Lawrence Berkeley Laboratory
Berkeley, CA 94720 USA

November 1990

THE REACTIONS OF GROUND STATE AND ELECTRONICALLY EXCITED SODIUM ATOMS WITH METHYL BROMIDE AND MOLECULAR CHLORINE

P. S. Weiss,[a] J. M. Mestdagh,[b] H. Schmidt,[c] M. H. Covinsky, and Y. T. Lee*

Department of Chemistry

University of California, Berkeley, and

Chemical Sciences Division

Lawrence Berkeley Laboratory

Berkeley, CA 94720

USA

Abstract

The reactions of ground and excited state Na atoms with methyl bromide (CH_3Br) and chlorine (Cl_2) have been studied using the crossed molecular beams method. For both reactions, the cross sections increase with increasing electronic energy. The product recoil energies change little with increasing Na electronic energy, implying that the product internal energies increase substantially. For $Na+CH_3Br$, the steric angle of acceptance opens with increasing electronic energy.

---

[a]Permanent Address: Department of Chemistry, The Pennsylvania State University, University Park, PA 16802, USA.
[b]Permanent Address: CEN Saclay, SPAS Bt. 62, 91191 Gif sur Yvette, France.
[c]Permanent Address: Braun A. G. Forschung, Frankfurter Str. 145, D6242 Kronberg, Federal Republic of Germany.

I. Introduction

The reactions of ground state alkali atoms (M) with halogen–containing molecules (RX) have been extensively studied for more than 50 years.[1-27] The present work is a continuation of the systematic study we have undertaken of the reactivity of excited Na atoms.[2-7] The aim is to determine the changes in the reaction dynamics when electronic energy is deposited in a reactant, here the Na atom. In this paper, we study reactions which for ground state Na atoms are representative of rebound and stripping mechanisms; these are the reactions of Na with methyl bromide and chlorine molecules, respectively.
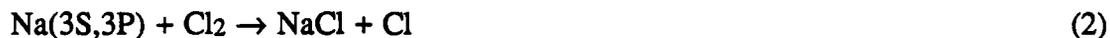
$$Na(3S,3P,4D) + CH_3Br \rightarrow NaBr + CH_3 \tag{1}$$

$$Na(3S,3P) + Cl_2 \rightarrow NaCl + Cl \tag{2}$$

For the reactions of ground state alkali atoms with halogen and methyl halide molecules the mechanism has an electron transferring from the alkali atom to the halogen–containing molecule. This electron goes into the lowest unoccupied molecular orbital which is an antibonding orbital of the R–X bond. For the methyl halide molecules this causes the rupture of this bond, as the negative ion is not bound. For the halogen molecules, the negative ion is formed on a repulsive part of the potential near the dissociation limit (to halide ion and halogen atom), and the field of the alkali ion is strong enough to dissociate the halogen negative ion.[8,9] Of the methyl monohalides, only the reactions of alkali atoms with CH_3I and CH_3Br have been studied in crossed molecular beams including the reactions of all the stable alkali metals with CH_3I.[10]

II. Experimental

As described previously, these experiments were conducted in a crossed molecular beams apparatus in which supersonic atomic sodium and molecular chlorine or methyl bromide beams crossed at 90°, and scattered products were detected with an ultrahigh vacuum mass spectrometer equipped with an electron bombardment ionizer which rotates about the interaction region.[2-5] In addition, one or two single frequency cw dye lasers optically pumped the Na atoms to the $Na(3^2P_{3/2}, 4^2D_{5/2})$ levels in the interaction region.[2-5]

The atomic and molecular beam conditions are given in table I. The Na atomic velocity distributions were measured by the laser technique described in refs. 4 and 5. The molecular beam velocity distributions were measured by the time–of–flight technique using a mass spectrometer.

III. Other Possible Processes

III.A. Na + CH3Br

A number of processes other than (1) are possible in the collisions of electronically excited Na with CH₃Br as discussed below.

Gersh and Bernstein have discussed energetically possible products in high energy (>1 eV) collisions of K+CH₃I,[11] and several of these endoergic processes, *mutatis mutandis*, are energetically possible here:

$$Na + CH_3Br \rightarrow CH_3Na + Br \qquad \Delta H_o^o = 26 \text{ kcal/mole}[28] \qquad (3)$$

$$Na + CH_3Br \rightarrow NaH + CH_2Br \qquad \Delta H_o^o = 59 \text{ kcal/mole}[30] \qquad (4)$$

$$Na + CH_3Br \rightarrow NaH + CH_2 + Br \qquad \Delta H_o^o = 66.2 \text{ kcal/mole}[33] \qquad (5)$$

$$Na + CH_3Br \rightarrow Na^+ + CH_3Br^- \qquad \Delta H_o^o = 103.5 \text{ kcal/mole}[34] \qquad (6)$$

$$Na + CH_3Br \rightarrow Na^+ + CH_3 + Br^- \qquad \Delta H_o^o = 107.3 \text{ kcal/mole}[38] \qquad (7)$$

Processes (3–7) are all substantially endothermic, but with the electronic excitation to Na(4D), 98.8 kcal/mole, and the collision energy of over 20 kcal/mole, all are energetically possible.

It is unlikely that significant amounts of methylsodium and sodium hydride are formed via processes (3) and (4) because these channels would require the Na to approach the methyl end of the methyl bromide molecule. As has been shown for K+CH₃I, there is a substantial repulsion for the alkali approaching the methyl end of the methyl halide in the ground state potential,[12] and this is certain to hold for the excited state potentials as well. No evidence is seen for CH₃Na nor for NaH, although these molecules are also expected to be observed at m/q=23 (Na⁺).

It is possible that at high collision energy the Na could dissociate the CH3Br as in process (5). This is most likely to happen where NaBr is produced above its dissociation limit (to atoms).

The present experiments are not arranged to detect the production of ions as in processes (6–7). Furthermore, CH_3Br^- has such a small potential well (3.8 kcal/mole), offset significantly from the equilibrium geometry of the neutral,[36] that it is extremely unlikely that it could be produced. However it is quite possible that the Na^+–Br^- ion pair could be produced via process (7). This is equivalent to the process seen by Lacmann and Herschbach for K+HCl.[13] As interpreted by Balint–Kurti and Yardley highly vibrationally excited KCl is produced above the dissociation limit to ions.[14]

It is also possible that some collisions quench the electronic excitation:

$$Na(nL) + CH_3Br \rightarrow Na(n'L') + CH_3Br \qquad (8)$$

Although process (8) certainly occurs, the present experiments are insensitive to it. In conclusion, only process (1) is detected in our experiments.

III.B. Na+Cl2

A number of other products are also energetically possible in the Na+Cl2 collisions:

$$Na + Cl_2 \rightarrow Na + Cl + Cl \qquad\qquad \Delta H_o^\circ = 58 \text{ kcal/mole}[39] \qquad (9)$$

$$Na + Cl_2 \rightarrow Na^+ + Cl_2^- \qquad\qquad \Delta H_o^\circ = 63.4 \text{ kcal/mole}[40] \qquad (10)$$

Processes (5) and (9) are analogous to the products found for K+HCl reaction by Lacmann and Herschbach and discussed above.[13,14]

Although we did not investigate processes involving ion production, it is expected that some charge transfer takes place (10) as seen for the energetic collisions of ground state species in ref. 15. At higher collision energies dissociative charge transfer similar to process (7) is also possible.

As with Na*+CH3Br, it is likely that some collisions simply quench the electronic excitation:

$$Na(nL) + Cl_2 \rightarrow Na(n'L') + Cl_2 \qquad\qquad (11)$$

However, if the long distance electron transfer from sodium atoms to chlorine molecules is the dominant process, the formation of product NaCl should be far more important than the quenching of electronic excitation. Only process (2) is detected in our experiments.

IV. Results

IV.A. Na(3S,3P,4D)+CH₃Br

The reaction:

$$Na + CH_3Br \rightarrow NaBr + CH_3 \qquad\qquad \Delta H_o^o = -20.7 \text{ kcal/mole}[33] \qquad (12)$$
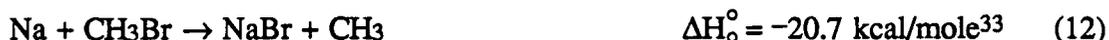
was studied at a collision energy of 21 kcal/mole for Na(3S,3P,4D) as shown in the angular distributions in fig. 1. Note that the data were recorded at m/q=23 (Na⁺) and thus include both reactive NaBr contributions (due to fragmentation in the electron bombardment ionizer) and non–reactive contributions from elastically and inelastically scattered Na atoms. The non–reactive scattering peaks at 0° and drops off rapidly as a function of angle as shown by the dashed line in fig. 1. The reactive scattering peaks at higher angles. The data show qualitatively similar angular distributions for the reactions of each of the three Na levels. The only difference between the distributions due to the Na(3S) and Na(3P) states appears to be on the small angle side of the reactive peak. This difference is more pronounced for the reactive scattering of the Na(4D) atoms. This region of the angular distribution for Na(3S,3P)+CH₃Br was expanded over the useful range of the detector by seeding the CH₃Br in helium, as shown in the NaBr product angular distribution (or more accurately *partial* angular distribution) recorded at a collision energy of 25 kcal/mole in fig. 2. The same behavior is exhibited in that the signal for Na(3P)+CH₃Br remains higher than for Na(3S)+CH₃Br in this region. The signal to noise ratio was too poor and the differences between the scattering intensities of the various Na states were too small to allow the measurement of time–of–flight and atomic alignment dependences as described in refs. 3 and 6, although these would certainly be of interest.

An attempt was made to measure the differential cross section of:

$$Na + CH_3Cl \rightarrow NaCl + CH_3 \qquad\qquad \Delta H_o^o = -13.5 \text{ kcal/mole}[41] \qquad (13)$$

Although some reactive scattering signal was observed, cross sections were too small to allow the measurement of laboratory angular distributions.

IV.B. Na(3S,3P)+Cl₂

Angular distributions of the NaCl product for the exothermic reaction:

$$Na(3S,3P) + Cl_2 \rightarrow NaCl + Cl_2 \qquad\qquad \Delta H_o^o = -40.4 \text{ kcal/mole}[39] \qquad (14)$$

were recorded at collision energies of 3, 6, and 19 kcal/mole. The angular distributions for a collision energy of 6 kcal/mole are shown in fig. 3. The three main features of the distributions are: 1) the shape of the distributions change very little in going to higher electronic energy, 2) the cross sections increase in going to higher electronic energy, and 3) the angular distributions are very narrow compared to the possible product NaCl angular ranges shown in the Newton diagram in the figure. The results for collision energies of 3 and 19 kcal/mole were very similar.[4,7]

Due to the small difference in the angular distributions between ground and excited states, no time–of–flight product velocity measurements, nor any laser polarization dependences were measured.

V. Analysis of Experimental Results

V.A. Na+CH₃Br

An iterative forward convolution method was used to fit independent center–of–mass (CM) scattering angular and CM translational energy distributions to the laboratory frame data.[42] In spite of the absence of information on the product velocity distributions, the ranges of the CM distributions which fit the laboratory angular distributions are rather narrow due the back–scattering of the Na+CH₃Br reaction. Because of the poor signal–to–noise ratios in the angular distributions and the similarities between the angular distributions for different Na

electronic states, rather than try to subtract the already noisy distributions, the raw data shown in fig. 1 was used to represent the data for each level excited. This has the effect of *underestimating* the differences in the scattering of the different states, but would still point out the trends in the reactivity.

The best fits to the angular distributions are shown as the solid lines in fig. 4. The CM angular and recoil energy distributions are shown in figs. 5 and 6, respectively, for Na(3S,3P,4D)+CH3Br. Some features of the fits are given in table II. The relative cross sections have been corrected for the estimated excitation fractions from ref. 3 — Na(3P) and Na(4D) fractions of 20% and 16%, respectively, when the appropriate lasers illuminate the interaction region.

The reactive cross sections can be calibrated by using the small angle elastic scattering.[9] Briefly, the cross section of small angle elastic scattering is estimated by using the small angle approximation to the classical scattering due to a long range attractive potential, $(V(r)=C_6r^{-6})$.[43] Since CH3Br has a permanent electric dipole moment, there are two contributions to C_6 — a dispersive term, approximated by the Slater–Kirkwood formula,[9,44] and a dipole–induced dipole term, given by the Debye formula.[3,45] The two terms are added to give the total C_6 constant. For the dispersive portion, the polarizability of CH3Br was determined from the sum of the polarizabilities of its bonds.[45] This calculation is described in ref. 4, and gives C_6(Na(3S)–CH3Br)=9990 kcal/mole $Å^6$. From the increased polarizability of the Na(3P) atom $(\alpha(Na(3P))=53.6 \, Å^3$ vs. $\alpha(Na(3S))=24.5 \, Å^3)$[46] a higher van der Waals constant is derived for the excited state, C_6(Na(3P)–CH3Br)=16090 kcal/mole $Å^6$.[4]

The small angle elastic scattering can be approximated by:

$$\frac{\delta\sigma_{el}}{\delta\omega_{abs}} = 0.239 \, \frac{C_6^{1/3}}{E^{1/3}} \theta^{-7/3},$$ (15)

where E is the collision energy in kcal/mole, and θ is the CM scattering angle in radians.[43] This is shown for ground state scattering as the dashed line in fig. 1. Equation (15) is valid where $\sin\theta \sim \theta$. As in refs. 3 and 4, it was assumed that 20% of the Na atoms were excited to the 3P level.

The ratio of the detection efficiencies of NaBr and Na at m/q=23 (Na+) where both were detected is just the ratio of the ionization cross sections for Na and NaBr to Na+. While the ionization cross section of Na is known, the ionization cross section of NaBr must be estimated. This is done by taking the ionization cross section to be the ionization cross section of isoelectronic Kr times the ratio of the polarizabilities of the two species $(\alpha(NaBr)/\alpha(Kr))$.[3] If it is assumed that as for NaCl, 90% of the vibrationally excited molecules fragment upon ionization to Na+, then the ratio of the detection efficiencies for NaBr vs. Na is 1.6:1. The cross sections derived for the reactions of Na(3S,3P,4D) with CH3Br are shown in table III. The absolute cross sections are probably only good to within a factor of two, and are strongly dependent upon the excitation fraction assumed.

V.B. Na+Cl2

Although no laboratory velocity data were recorded, the predominance of the forward scattering and the narrow recoil energy distributions once again gave reliable approximate CM distributions from the relatively primitive laboratory angular distributions.[8,9,16,17]

The single CM angular distribution derived by Grice and Empedocles for K,Rb,Cs+Cl2 at collision energies under 1 kcal/mole[16] was unable to fit the measured angular distributions for Na+Cl2. The best fits to the laboratory angular distributions for Na(3S,3P)+Cl2 at a collision energy of 6 kcal/mole are shown in fig. 7. The CM angular distributions derived for these fits are shown in fig. 8. The recoil energy distributions derived are shown in fig. 9. A summary of the features of these fits is given in table IV. The CM angular distributions widen and the peak recoil energies increase for the reaction of Na(3P) as compared to Na(3S). Note that the column labeled "Fraction Forward Scattered" gives the fraction of the weighted intensity $T(\theta)\sin\theta$ that is in the forward hemisphere.

As in section V.A., the absolute reactive scattering cross sections were estimated by approximating the C_6 constant and then fitting the small angle elastic scattering. The value of C_6 used in this calculation, $C_6(Na(3S)-Cl_2)=7410$ kcal/mole $\mathring{A}^6$ is very close to the theoretical value derived by Anderson and Herschbach of $C_6(Na(3S)-Cl_2)=7460$ kcal/mole $\mathring{A}^6$.[18] Once again, a higher van der Waals constant was derived for the excited state, $C_6(Na(3P)-Cl_2)=11340$ kcal/mole $\mathring{A}^6$. As discussed in ref. 3, since little energy appears as product translational energy, it is safe to assume that the product NaCl is highly internally excited, and yields predominantly Na^+ in the ionization process. The relative detection efficiencies of internally excited NaCl and Na atoms were derived to be 1.8:1 in ref. 3. The results of the calibration of the absolute cross section for the data recorded at a collision energy of 6 kcal/mole are given in table V.

VI. Discussion

VI.A. Na+CH₃Br

With increasing electronic energy the reactive cross sections increase, the center–of–mass angular distributions widen, but the reaction still proceeds via the rebound mechanism. These results are discussed on the basis of features of the ground state Na atom reactions which have been known since the early days of crossed molecular beams scattering.

The first crossed molecular beams experiment on K+CH₃I revealed the rebound mechanism found in all subsequent experiments of the reactions of alkali atoms with alkyl monohalides.[19] The elegant work of Bernstein and coworkers,[20] and Brooks and coworkers[21] in orienting methyl halide molecules in a molecular beam prior to reaction confirmed the steric effect earlier ascribed to the reaction. That is, for small impact parameter collisions, if the alkali atom comes in at the halogen end of the molecule, then the reaction probability is unity. If the alkali atom approaches the methyl end of the molecule, then the reaction probability is zero.[19] The result of this steric effect is a backwards peaked angular distribution (with respect to the incoming alkali atom direction). The farthest back–scattered MX products (highest laboratory angles) correspond to the most collinear

C–X–M geometries. Smaller C–X–M approach angles correspond to smaller CM scattering angles.

The slightly widening CM angular distributions shown in fig. 7 (and table II) support the idea that an opening of the steric angle of acceptance for reaction occurs with increasing electronic energy and thus sodium orbital size. The less strict geometric requirements on the approach geometry lead to the broader CM angular distributions. This is visible in the raw data of fig. 1 as the increase in signal on the small angle side of the reactive peak. Near the maximum in the reactive scattering angular distributions, the intensity does not increase substantially upon excitation because the rebound collisions leading to scattering at these angles already have reaction probabilities near unity for ground state scattering.

The recoil energy distributions do not shift with changing electronic energy implying that ions released at a distance come together to form a vibrationally excited ionic molecule. This is as brought forth in the DIPR (Direct Interaction with Product Repulsion) model introduced by Kuntz, Mok, and Polanyi to treat the reactions of ground state alkali atoms with halogen and methyl halide molecules.[22] In this model only two interactions are considered; these are: $\{R-X\}^-$ and M^+-X^-. Furthermore, the DIPR model uses a fixed repulsive energy release to determine the translational energy release in the reaction. The difference in treatment of the two reactive systems is that for halogen molecules charge is allowed to migrate from one atom to the other, whereas for the alkyl halide this is not possible.

As the electron jump distance moves to larger separation for successively higher Na electronic states (with successively lower ionization potentials) the distance at which the Na^+-Br^- attraction takes over becomes larger, and the resultant NaBr molecule is produced in successively higher vibrational levels. A nearly vertical $CH_3Br+e^- \rightarrow CH_3Br^-$ transition takes place so that the translational energy released is essentially the same for each electronic state.

The ground state reactive cross sections determined for Na+CH3Br are of the same order as those determined in ref. 23 for K+CH3Br. This is expected as the dominant factor in the reactivity of alkali atoms with methyl halide molecules appears to be the choice of halogen atom. The orientation of the CH3Br plays a more important role than the variance in the covalent–ionic crossing distances for various Na electronic states.

VI.B. Na+Cl₂

With increasing electronic energy, the reactive cross section again increases, the angular distribution is less forward peaked, and the recoil energy increases substantially. Kuntz, Mok, and Polanyi have argued that the forward scattering observed for the reactions of ground state alkali atoms with halogen molecules are due to secondary encounters between the alkali atom and the departing halogen atom.[22] They based this on calculations using the DIPR model. As pointed out in ref. 22, this type of interaction violates two of the conditions of the model — that there be no interaction between the alkali atom and the departing fragment, and that the repulsive potential for the departing fragment be monotonically decreasing.

In the reactions of excited alkali atoms, the crossing point of the neutral and ionic potential surfaces moves further out. In this way the electron transfer initiating the reaction should occur at larger separation, giving the halogen ion time to dissociate before the arrival of the alkali ion. This should *reduce* the number of secondary encounters, and as a consequence, the products of the excited state reactions should be less forward scattered. This is what is observed experimentally.

A second prediction of the DIPR model is that similar recoil distributions should be obtained for each Na electronic state since the X_2^- repulsion remains the same. In order to conserve total energy, this must be associated with increasing product internal energies for increasing electronic energy. The product internal energies would be expected to increase simply because the coulombic M^+–X^- attraction begins at larger separation, thereby giving more vibrational and rotational energy to the MX molecule. This is similar to the effects observed in the reaction of Na(4D,5S)+HCl→NaCl+H in ref. 3. Here, however, the peak product recoil energy increases by a

factor of two in going from Na(3S) to Na(3P) at a collision energy of 6 kcal/mole. A larger *fraction* of the additional (electronic) energy deposited in the system does go into the product internal energies, as the total energy deposited has increased eightfold upon excitation of the Na atoms at this collision energy.

Finally the DIPR model predicts increasing cross sections with increasing Na electronic energy since the electron jump distance moves to larger values. While this is qualitatively consistent with the experimental results, the increase is smaller than the estimated electron transfer cross section $\sigma = \pi r_c^2$, where r_c is the radius at which the neutral and ionic curves cross. Using the vertical electron affinity of Cl_2, EA=0.7 eV,[47] the electron transfer (harpoon) cross sections calculated are given in table V. However, it has been shown that the electron transfer cross sections calculated from halogen vertical electron affinities are often too low.[24,25] The electron transfer cross sections estimated using the adiabatic electron affinity of Cl_2, EA=2.39 eV,[32] are also given in table V. That the increase in the reaction cross section is smaller than the increase in πr_c^2 implies that the covalent–ionic curve crossing probability is a strong function of impact parameter. We note that as the crossing point moves to larger separation and the crossing probability becomes smaller, the Cl_2 orientation may play an increasingly important role in determining the crossing and thus the reaction probability.

Maya and Davidovitz have measured the cross sections of the reactions of alkali atoms with halogen molecules at thermal energies in a gas cell.[25,26] For $Na+Cl_2$ at a mean collision energy of 1.6 kcal/mole, they measured σ_R=124 Å^2 with a reported accuracy of ±15%.[25] By comparison, the average of the two values obtained here for the ground state at a collision energy of 6 kcal/mole, σ_R=70 Å^2 is qualitatively consistent with a drop off of the reactive cross section with increasing collision energy as reported in ref. 27. The limited accuracy of the current measurements prevents a quantitative comparison.

VII. Conclusions

The most striking feature of the reactions of the various states of Na with Cl_2 and CH_3Br is their similarity. In both reactions, the reactivity increases somewhat with increasing electronic energy. In both reactions, the product recoil energy does not change with increasing electronic energy implying that the product internal energy increases substantially. In contrast to Na+HCl,[3] no major change in reaction dynamics is observed upon excitation to different electronic states. This confirms that the dynamics in these two systems are determined by the lowest unoccupied molecular orbital of the halogen–containing molecule.

The rebound mechanism describes the reactions of the ground and excited states of Na with CH_3Br. Besides the increasing cross sections, the main difference in the reaction dynamics appears to be that the steric angle of acceptance opens somewhat for higher electronic states, and thus for larger, more diffuse electronic orbitals.

In the reaction of Na with Cl_2, the cross section does not increase nearly as much with increasing electronic energy as would have been predicted from simple harpoon arguments. The reactive cross sections are in qualitative agreement with a reduced electron transfer probability due to a smaller interaction at the larger separations at which electron transfer becomes energetically possible.

Acknowledgments

Table I. Measured atomic and molecular beam velocities and speed ratios.

Beam	Seed Gas	Beam Velocity (in cm/sec)	Speed Ratio (v/Δv FWHM)
Na	Helium	3.00×10^5	6
Na	Neon	1.60×10^5	5
Na	Argon	1.08×10^5	5
Cl_2	–	6.1×10^4	5
CH_3Br	–	5.8×10^4	5
CH_3Br	Helium	1.26×10^5	4

Table II. Features of the center–of–mass distributions of the $Na(3S,3P,4D)+CH_3Br$ reaction at a collision energy of 21 kcal/mole.

Na Level	FWHM of T(θ)	Fraction Backwards Scattered	Peak Recoil Energy (in kcal/mole)	σ(nL)/σ(3S)
3S	73°	0.84	33	1.0
3P	74°	0.84	33	1.6
4D	83°	0.79	33	2.8

Table III. Estimated total reaction cross sections for $Na(3S,3P,4D)+CH_3Br$ at a collision energy of 21 kcal/mole from the elastic scattering of $Na(3S,3P)$ atoms and estimates of the absolute cross sections from Van der Waals attraction of the indicated states.

Electronic State	Reactive Scattering Cross Sections	
	from Na(3S)	from Na(3P)
3S	6 Å²	6
3P	9 Å²	9 Å²
4D	16 Å²	16 Å²

Table IV. Features of the center–of–mass distributions of the Na(3S,3P)+Cl$_2$ reaction at a collision energy of 6 kcal/mole.

Na Level	FWHM of T(θ)	Fraction Forward Scattered	Peak Recoil Energy (in kcal/mole)	$\sigma(nL)/\sigma(3S)$
3S	76°	0.83	0.6	1.0
3P	97°	0.76	1.2	1.58

Table V. Estimated total reaction cross sections for Na(3S,3P)+Cl$_2$ at a collision energy of 6 kcal/mole from the elastic scattering of Na(3S,3P) atoms and estimates of the absolute cross sections from Van der Waals attraction of the indicated states. Also, harpoon cross sections calculated from the vertical and adiabatic Cl$_2$ electron affinities.

Electronic State	Reactive Scattering Cross Section from Na(3S)	from Na(3P)	Harpoon Cross Section from Vertical Electron Affinity	from Adiabatic Electron Affinity
3S	80 Å^2	60 Å^2	32 Å^2	86 Å^2
3P	120 Å^2	110 Å^2	121 Å^2	1560 Å^2

REFERENCES

1.   Polanyi, M. *Atomic Reactions*; Williams and Northgate: London, 1932.

2.   Vernon, M. F.; Schmidt, H.; Weiss, P. S.; Covinsky, M. H.; Lee, Y. T. *J. Chem. Phys.*
      1986, *84*, 5580.

3.   Weiss, P. S.; Mestdagh, J. M.; Covinsky, M. H.; Balko, B. A.; Lee, Y. T. *Chem. Phys.*
      1988, *126*, 93.

4.   Weiss, P. S. Ph.D. Dissertation, University of California, Berkeley, California, 1986.

5.   Vernon, M. F. Ph.D. Dissertation, University of California, Berkeley, California, 1983.

6.   Weiss, P. S.; Covinsky, M. H.; Schmidt, H.; Balko, B. A.; Lee, Y. T.; Mestdagh, J. M.
      Z. *Phys. D* **1988,** *10*, 227.

7.   Mestdagh, J. M.; Balko, B. A.; Covinsky, M. H.; Weiss, P. S.; Vernon, M. F.; Schmidt, H.;
      Lee, Y. T. *Faraday Disc. Chem. Soc.* **1987,** *84*, 145.

8.   Birely, J. H.; Herschbach, D. R. *J. Chem. Phys.* **1966,** *44*, 1690.

9.   Birely, J. H.; Herm, R. R.; Wilson, K. R.; Herschbach, D. R. *J. Chem. Phys.* **1967,** *47*, 993.

10.   Herm, R. R. In *Alkali Halide Vapors: Structure, Spectra, and Reaction Dynamics*;
      Academic Press: New York, 1979; Chapter 6 and references therein.

11.   Gersh, M. E.; Bernstein, R. B. *J. Chem. Phys.* **1972,** *56*, 6131.

12.   Raff, L. M.; Karplus, M. *J. Chem. Phys.* **1966,** *44*, 1212 and references therein.

13.   Lacmann, K.; Herschbach, D. R. *Chem. Phys. Lett.* **1970,** *6*, 106.

14.   Balint–Kurti, G. G.; Yardley, R. N. *Faraday Disc. Chem. Soc.* **1977,** *62*, 77.

15.   Aten, J. A.; Los, J. *Chem. Phys.* **1977,** *25*, 47; Los, J.; Kleyn, A. W. In *Alkali Halide
      Vapors: Structure, Spectra, and Reaction Dynamics*; Academic Press: New York, 1979;
      Chapter 8.

16.   Grice, R.; Empedocles, P. *J. Chem. Phys.* **1968,** *48*, 5352.

17.   Parrish, D. D.; Herm, R. R. *J. Chem. Phys.* **1969,** *51*, 5467; Grosser, A. E.; Bernstein, R. B.
      J. Chem. Phys. **1965,** *43*, 1140.

18.   Anderson, R. W.; Herschbach, D. R. *J. Chem. Phys.* **1975,** *62*, 2666.

19.   Herschbach, D. R.; Kwei, G. H.; Norris, J. A. *J. Chem. Phys.* **1961,** *34*, 1842.

20.   Parker, D. H.; Chakravorty, K. K.; Bernstein, R. B. *J. Chem. Phys.* **1981**, *85*, 466.

21.   Marcelin, G.; Brooks, P. R. *J. Am. Chem. Soc.* **1975**, *97*, 1710.

22.   Kuntz, P. J.; Mok, M. H.; Polanyi, J. C. *J. Chem. Phys.* **1969**, *50*, 4623.

23.   Goldbaum, R. H.; Robbin Martin, L. *J. Chem. Phys.* **1975**, *62*, 1181.

24.   Davidovitz, P. In *Alkali Halide Vapors: Structure, Spectra, and Reaction Dynamics*; Academic Press: New York, 1979; Chapter 9.

25.   Maya, J.; Davidovitz, P. *J. Chem. Phys.* **1974**, *61*, 1082.

26.   Maya, J.; Davidovitz, P. *J. Chem. Phys.* **59**, 3143 (1973).

27.   Gillen, K. T.; Rulis, A. M.; Bernstein, R. B. *J. Chem. Phys.* **1971**, *54*, 2831; Whitehead, J. C.; Hardin, D. R.; Grice, R. *Mol. Phys.* **23**, 787 (1972); Lin, S.-M.; Mascord, D. J.; Grice, R. *Mol. Phys.* **1974**, *28*, 975; van der Meulen, A.; Rulis, A. M.; deVries, A. E. *Chem. Phys.* **1975**, *7*, 1.

28.   Calculated from the H_3C-Br dissociation energy (66.2 kcal/mole) in ref. 29, and an estimated $Na-CH_3$ bond strength of 40 kcal/mole.

29.   van Veen, G. N. A. Ph.D. Dissertation, Rijksuniversiteit te Utrecht, Utrecht, The Netherlands, 1984.

30.   Calculated from the $H-CH_2Br$ dissociation energy (102 kcal/mole) in ref. 31, and the D_o^o value for NaH (43 kcal/mole) given in ref. 32.

31.   *CRC Handbook of Chemistry and Physics*, 65th ed.; CRC Press: Boca Raton, 1984.

32.   Huber, K. P. ; Herzberg, G. *Molecular Spectra and Molecular Structure, IV. Constants of Diatomic Molecules*; Van Nostrand Reinhold, Co.: New York, 1979.

33.   Calculated from the H_3C-Br dissociation energy (66.2 kcal/mole) in ref. 29, and the D_o^o value for NaBr (86.9 kcal/mole) given in ref. 32.

34.   Calculated from the ionization potential of Na (118.5 kcal/mole) in ref. 35, the H_3C-Br^- bond strength (3.8 kcal/mole) in ref. 36, and the electron affinity of Br (77.4 kcal/mole) in ref. 37.

35.   Wiese, W. L.; Smith, M. W.; Miles, B. M. *Atomic Transition Probabilities Volume II: Sodium Through Calcium, Natl. Std. Ref. Data Series*; National Bureau of Standards (U.S.): Washington, D.C., 1967.

36.   Wentworth, W. E.; George, R.; Keith, H. *J. Chem. Phys.* **1969**, *51*, 1791.

37.   Berry, R. S.; Riemann, C. W. *J. Chem. Phys.* **1963**, *38*, 1540.

38.   Calculated from the ionization potential of Na (118.5 kcal/mole) in ref. 35, the H_3C-Br dissociation energy (66.2 kcal/mole) in ref. 29, and the electron affinity of Br (77.4 kcal/mole) in ref. 37.

39.   Calculated from the diatomic molecular dissociation constants (D_o^o) given in ref. 32.

40.   Calculated from the ionization potential of Na (118.5 kcal/mole) in ref. 35, and the electron affinity of Cl_2 (55.1 kcal/mole) in ref. 32.

41.   Calculated from the H_3C-Cl dissociation energy (84.0 kcal/mole) in ref. 31, and the D_o^o value for NaCl (97.5 kcal/mole) given in ref. 32.

42.   Buss, R. J. Ph.D. Dissertation, Univ. of California, Berkeley, California (1979).

43.   Mason, E. A.; Vanderslice, J. T.; Raw, C. J. G. *J. Chem. Phys.* **1964**, *40*, 2153.

44.   Slater, J. C.; Kirkwood, J. G. *Phys. Rev.* **1931**, *37*, 682; K. Pitzer, *Adv. Chem. Phys.* **1959**, *2*, 59.

45.   Hirschfelder, J. O.; Curtiss, C. F.; Bird, R. B. *Molecular Theory of Gases and Liquids*; John Wiley and Sons: New York, 1964.

46.   Werner, H.–J.; Meyer, W. *Phys. Rev. A* **1976**, *13*, 13; Hannaford, P.; MacGillivray, W. R.; Standage, M. C. *J. Phys. B: Atom. Molec. Phys.* **1979**, *12*, 4033; Duong, H. T.; Pique, J.–L. *J. Physique* **1972**, *33*, 513.

47.   Gilbert, T. L.; Wahl, A. C. *J. Chem. Phys.* **1971**, *55*, 5247.

FIGURE CAPTIONS

Fig. 1. a) Newton diagram for Na(3S,3P,4D)+CH₃Br at a collision energy of 21 kcal/mole.
b) Measured angular distributions for Na(3S,3P,4D)+CH₃Br at a collision energy of 21 kcal/mole.

Fig. 2. Measured angular distributions for Na(3S,3P)+CH₃Br at a collision energy of 25 kcal/mole.

Fig. 3. a) Newton diagram for Na(3S,3P)+Cl₂ at a collision energy of 6 kcal/mole.
b) Measured angular distributions for Na(3S,3P)+Cl₂ at a collision energy of 6 kcal/mole.

Fig. 4. Fits of the angular distributions for Na(3S,3P,4D)+CH₃Br at a collision energy of 21 kcal/mole are shown as the solid curves and the experimental points are shown as circles for: a) Na(3S), b) Na(3P), and c) Na(4D).

Fig. 5. Center–of–mass angular distributions derived for the fits shown in fig. 4 for Na(3S,3P,4D)+CH₃Br at a collision energy of 21 kcal/mole.

Fig. 6. Recoil energy distributions derived for the fits shown in fig. 4 for Na(3S,3P,4D)+CH₃Br at a collision energy of 21 kcal/mole.

Fig. 7. Fits of the angular distributions for Na(3S,3P)+Cl₂ at a collision energy of 6 kcal/mole are shown as the solid curves and the experimental points are shown as circles.

Fig. 8. Center–of–mass angular distributions derived for the fits shown in fig. 7 for Na(3S,3P)+Cl₂ at a collision energy of 6 kcal/mole.

Fig. 9. Recoil energy distributions derived for the fits shown in fig. 7 for Na(3S,3P)+Cl₂ at a collision energy of 6 kcal/mole.

a)

38

V_{Na}
3.0×10^5 cm/sec

3S

3P

4D

V_{MeBr}
5.8×10^4 cm/sec

$\longmapsto$ 5.0×10^4 cm/sec

b)

Na(3S)
Na(3P)
Na(4D)

1

Signal (arb. units)

0.5

Na   cm   CH₃Br

0

0   30   60   90

Laboratory Angle (degrees)

XBL 863-874 A

Fig. 1

-21-

XBL 863-873

Fig. 2

a)

3P

3S   49

V_{Na}
1.6×10^5
cm/sec

V_{Cl_2}

6.1×10^4 cm/sec

⊢———⊣ 5.0×10^4 cm/sec

b)

○ Na(3S)
● Na(3P)

Signal (arb. units)

1

0.5

0

Na   cm Cl_2

0   30   60   90

Laboratory Angle (degrees)

XBL 863-865 A

Fig. 3

-23-

Fig. 4(a)

XBL 862-664

-24-
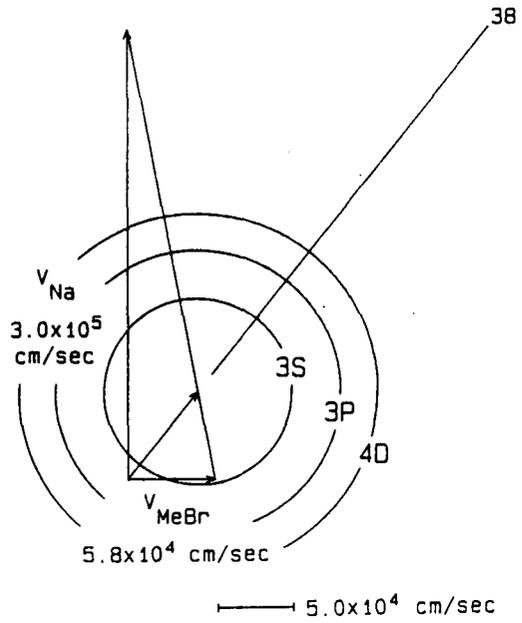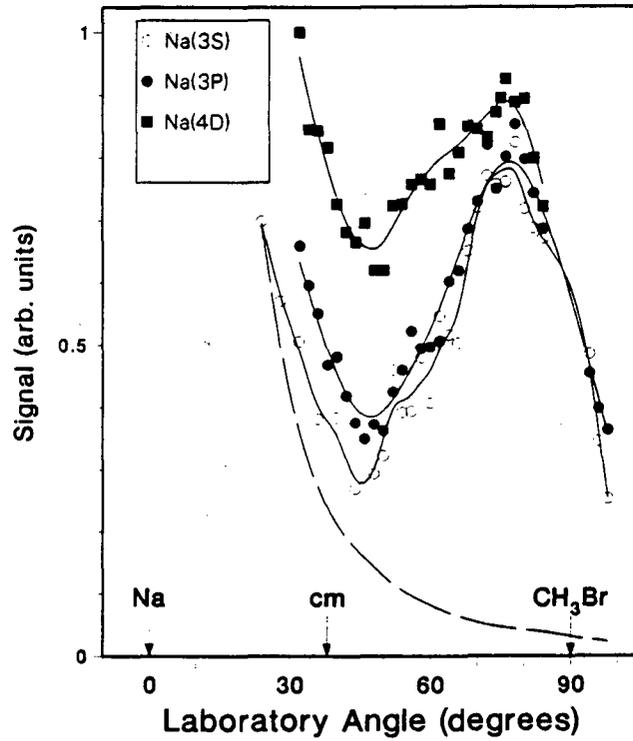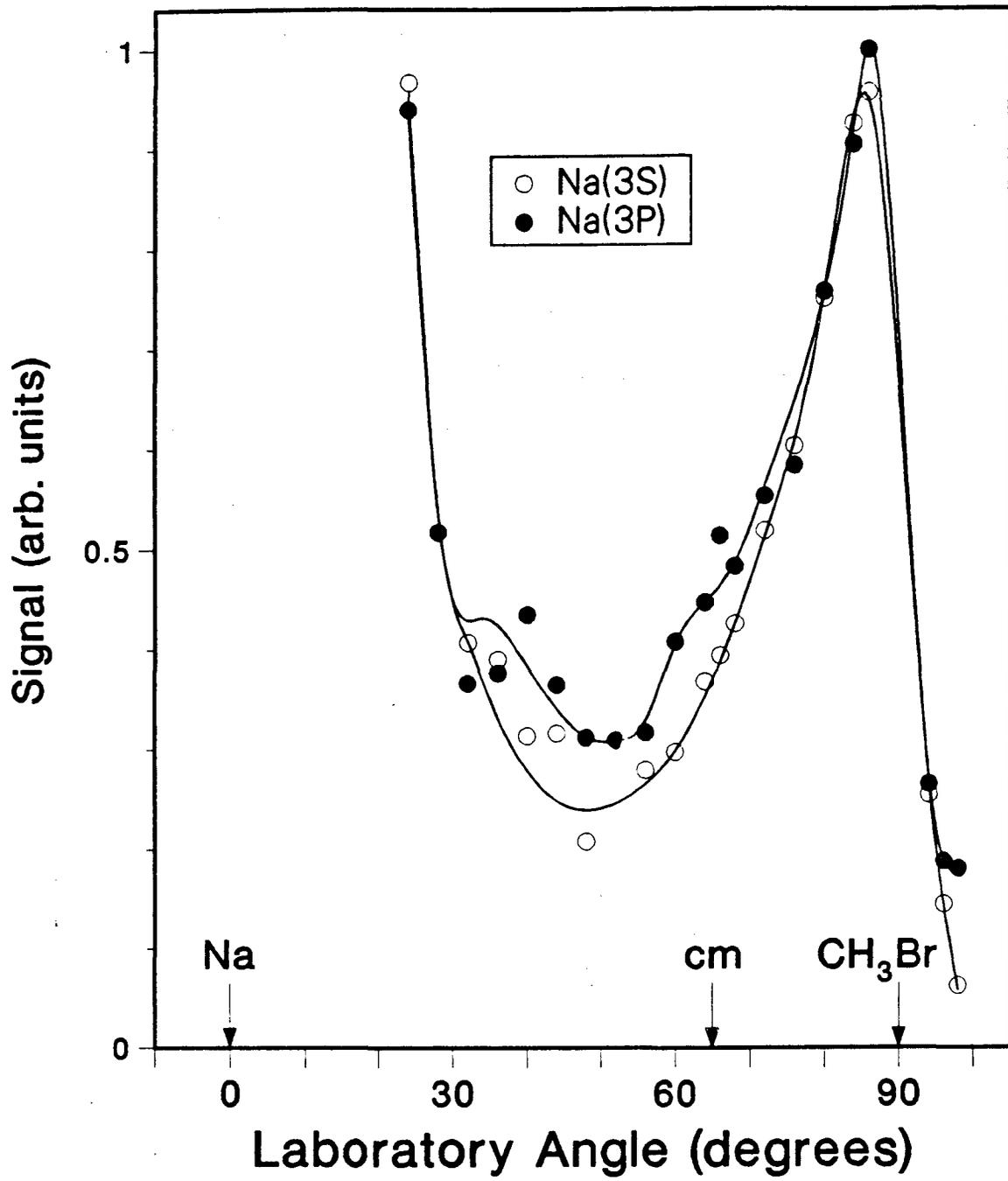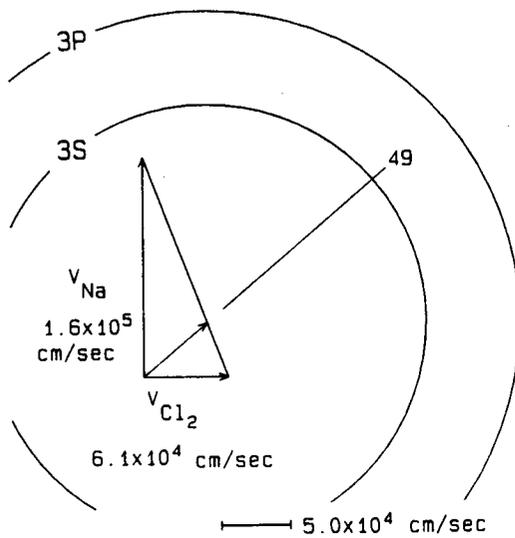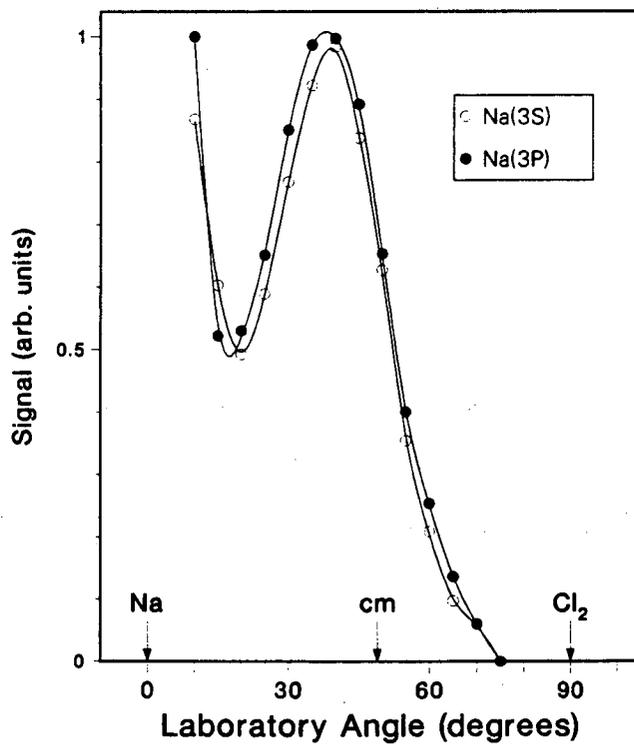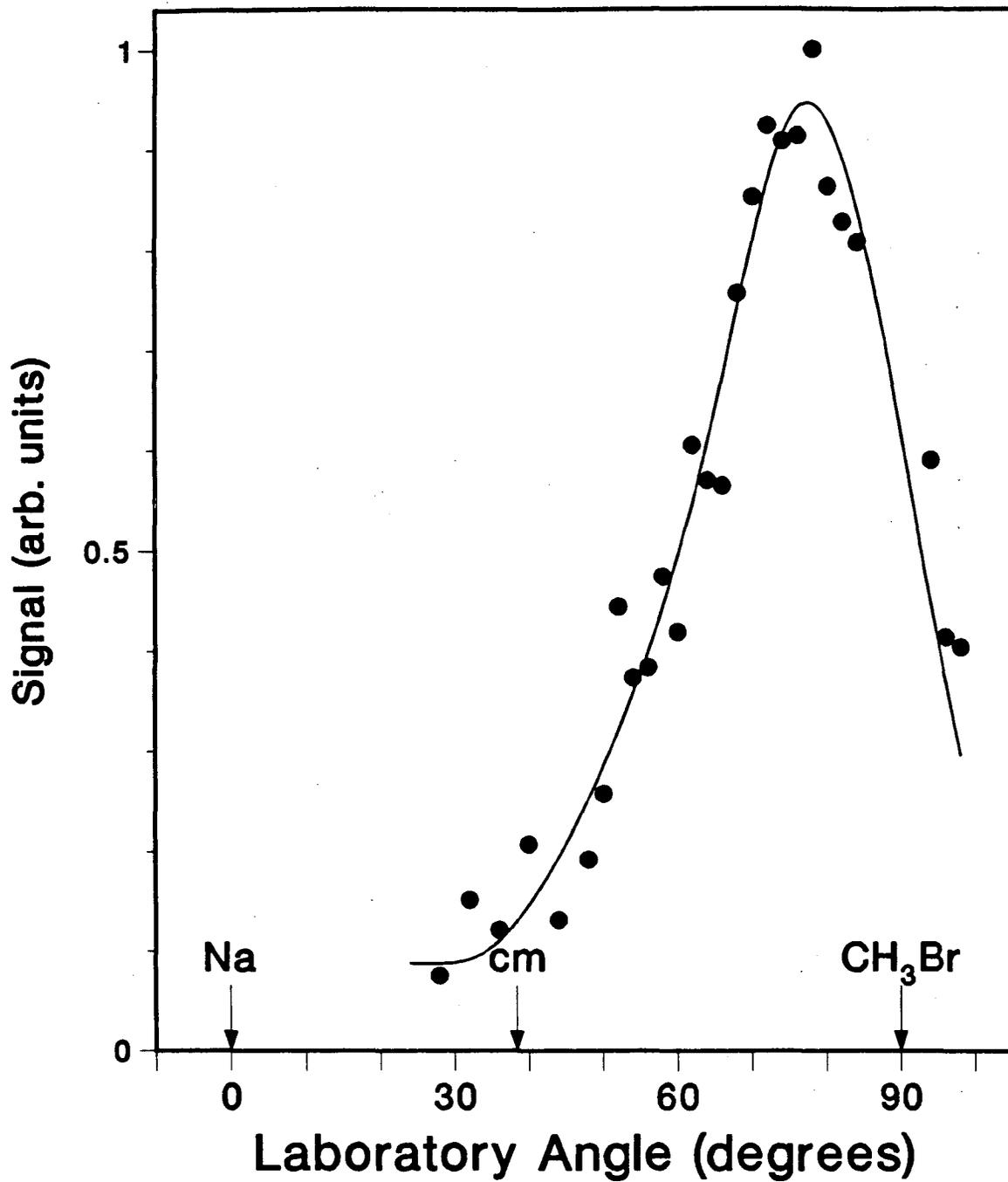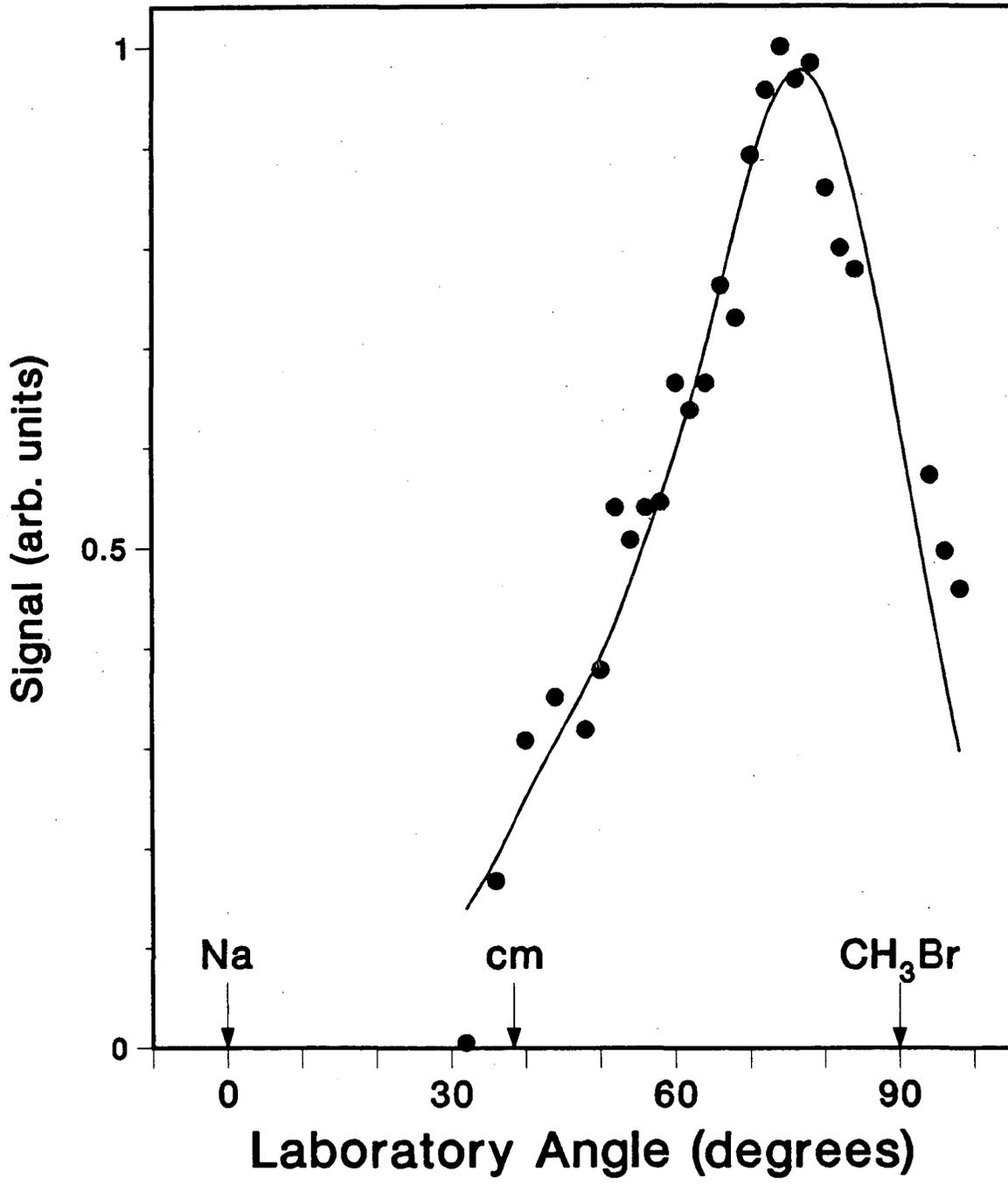
Fig. 4(b)
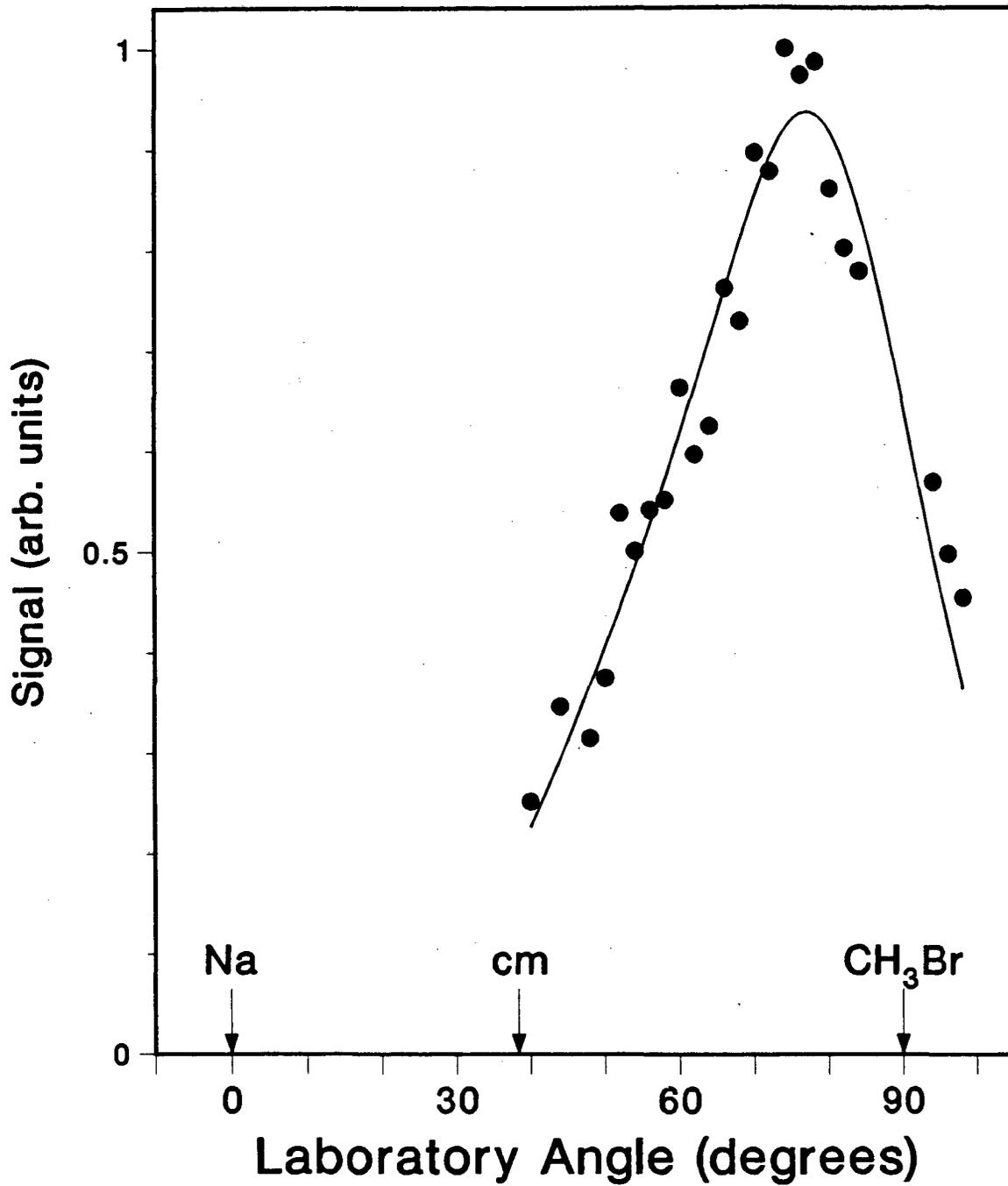
XBL 862-665

Fig. 4(c)
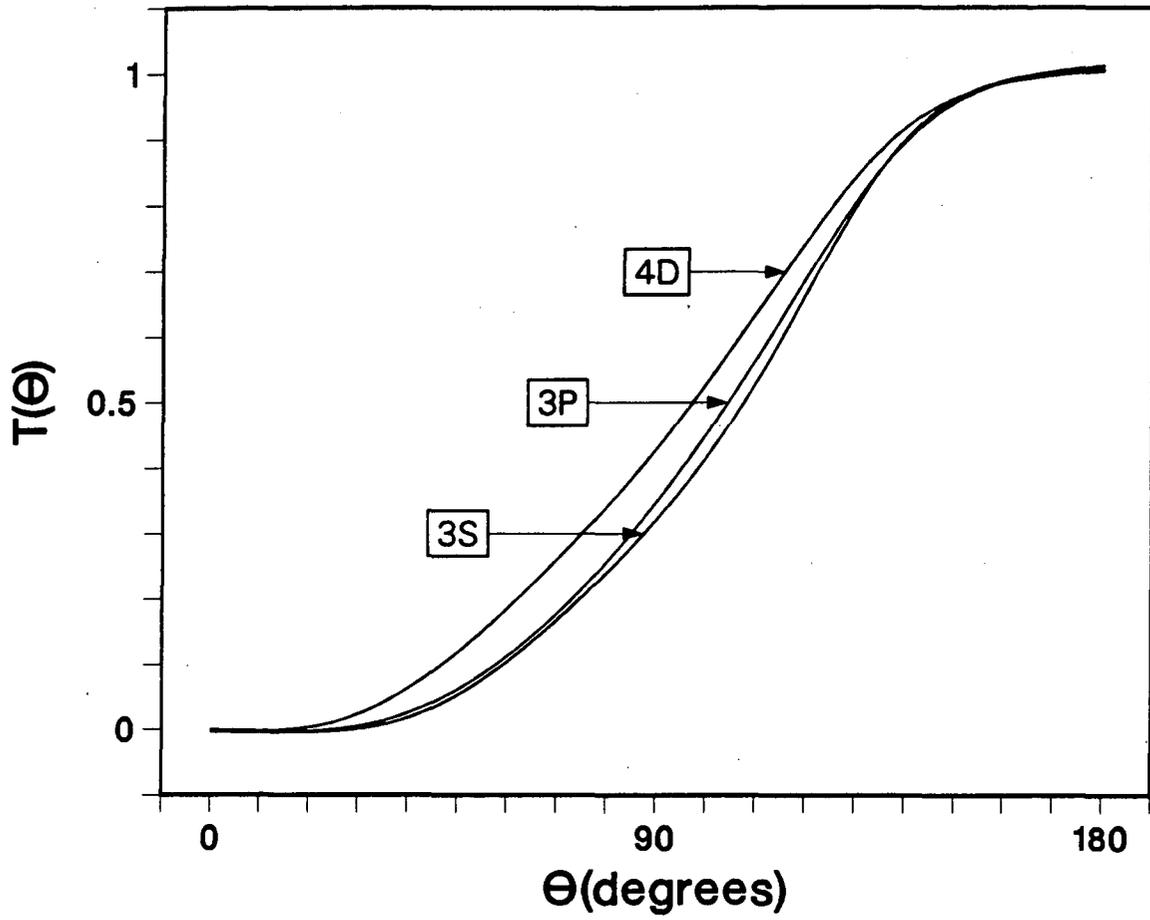
XBL 862-666

Fig. 5
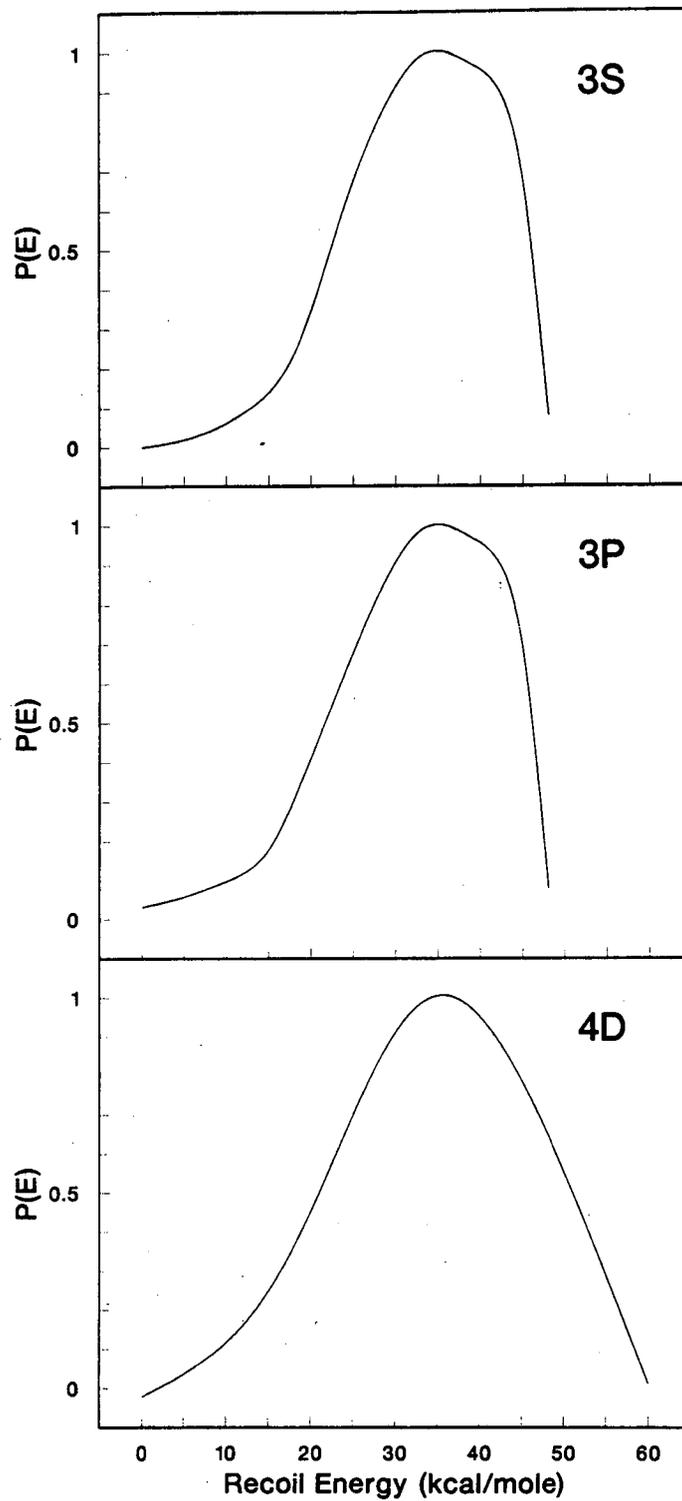
XBL 862-663

XBL 863-755

Fig. 6
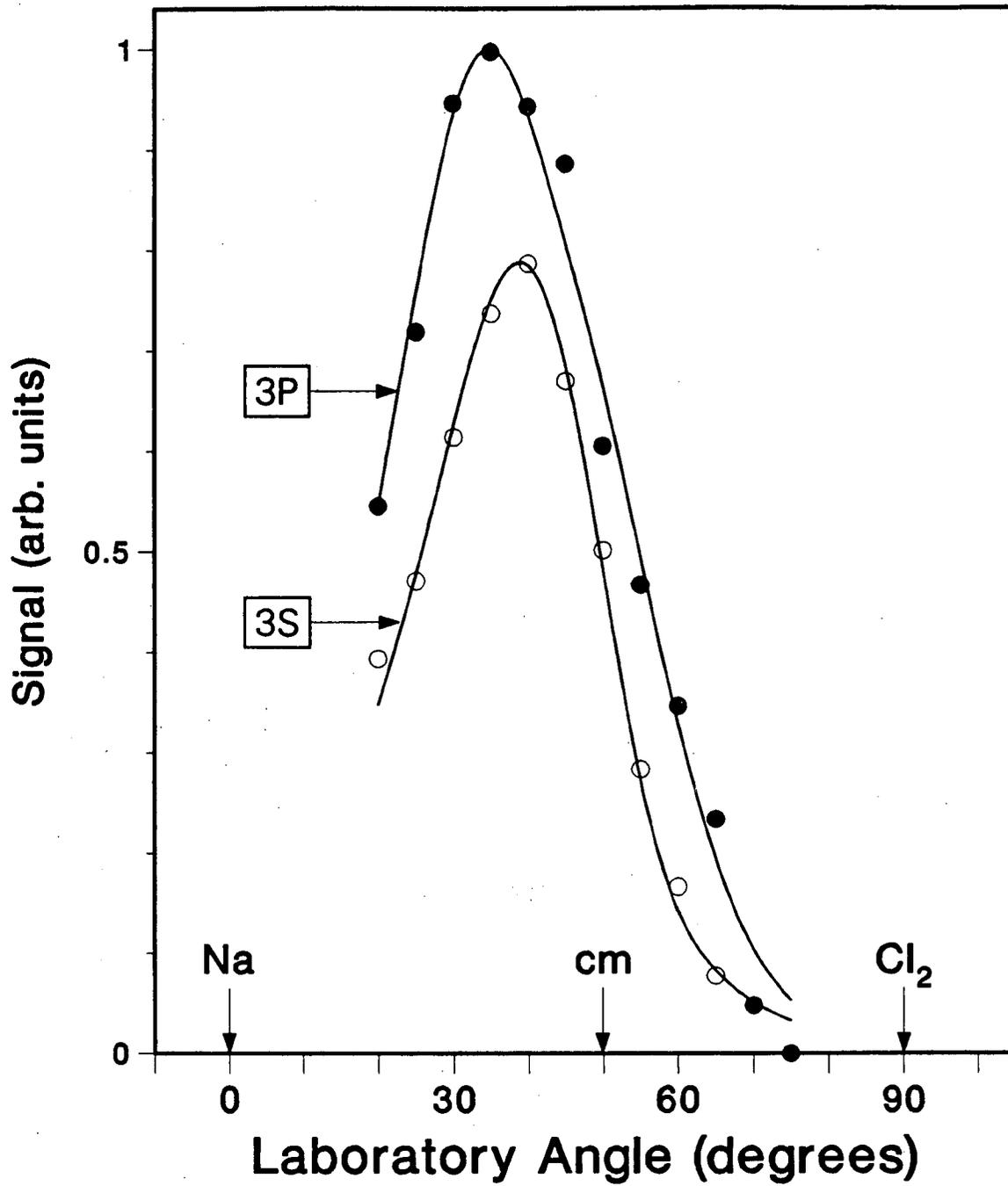
Fig. 7

XBL 862-559
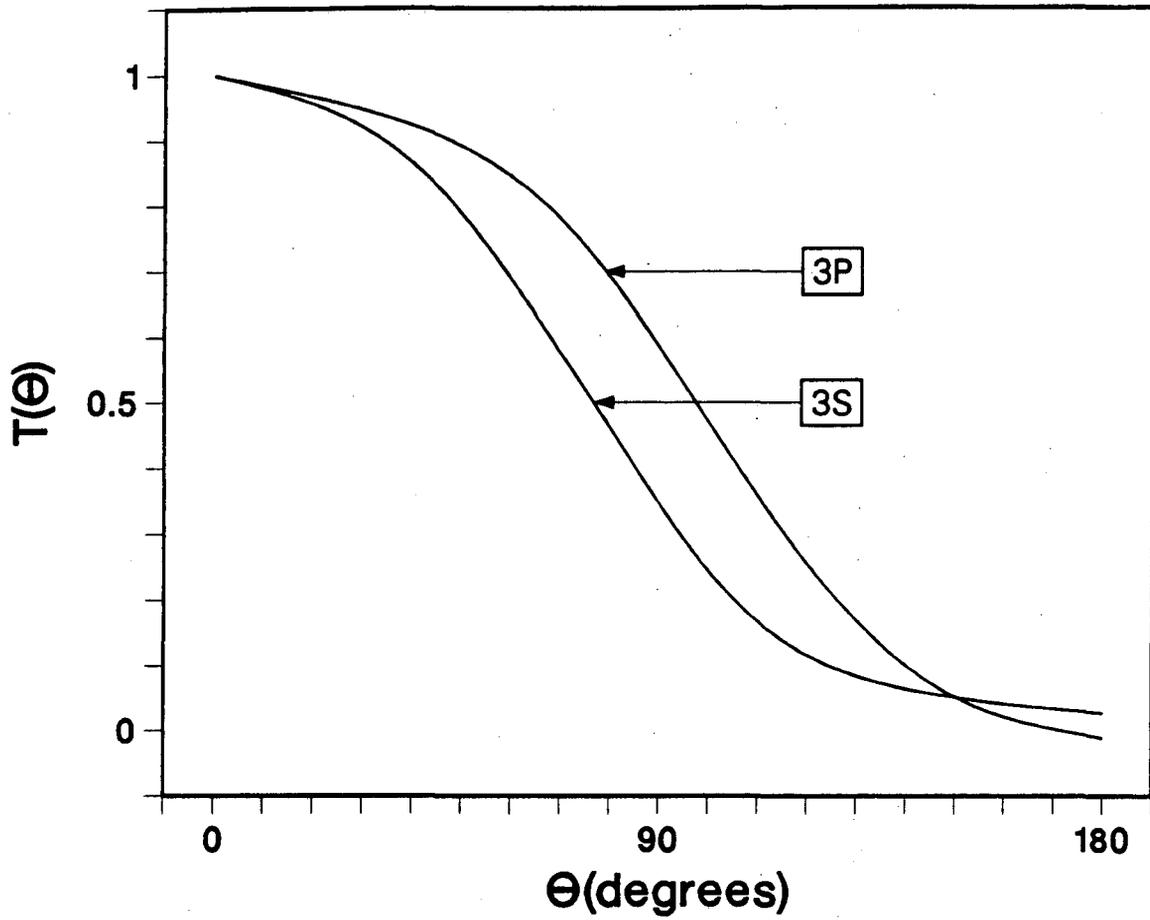
Fig. 8

XBL 862-662
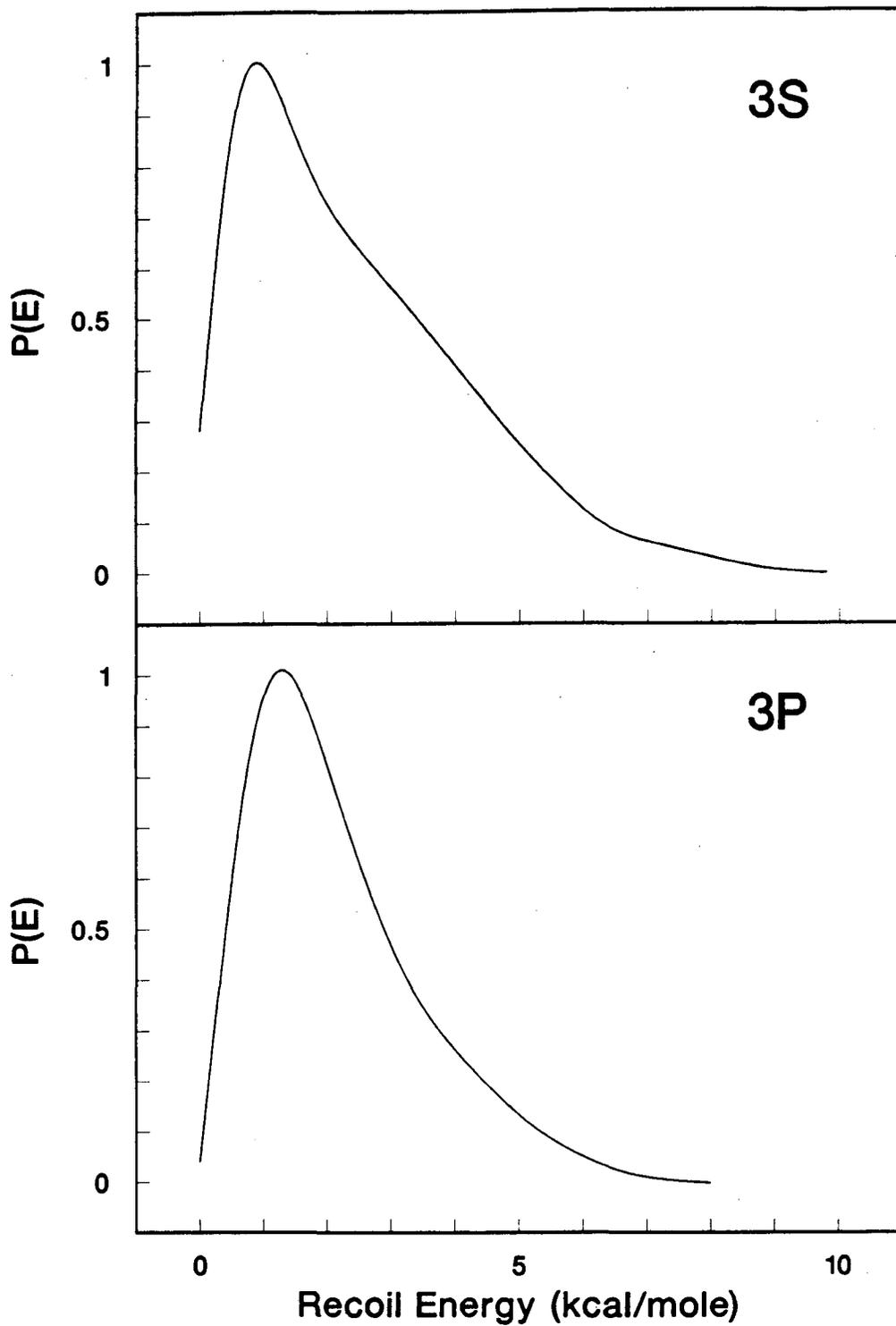
Fig. 9

XBL 863-753

LAWRENCE BERKELEY LABORATORY
UNIVERSITY OF CALIFORNIA
INFORMATION RESOURCES DEPARTMENT
BERKELEY, CALIFORNIA 94720